Open Access Journal
Journal of Power Technologies 94 (3) (2014) 153–164
journal homepage:papers.itc.pw.edu.pl

Methodology for choosing the optimum architecture of a STES system

Jarosław Milewski*, Marcin Wolowicz, Wojciech Bujalski

Institute of Heat Engineering
Warsaw University of Technology, 21/25 Nowowiejska Street, 00–665 Warsaw, Poland

Abstract

The paper presents a methodology for choosing geometrical parameters of a Seasonal Thermal Energy Storage facility (STES) on its thermal capacity. The STES is placed in both the ground under ground and connected to and solar panels. A number of scenarios were investigated to find an adequate geometrical proportions of the STES (for constant tank size and solar panel area.) The results obtained show that the use of various STES geometries could reduce heat accumulation to 30% depending on the architecture solution chosen.

Keywords: Seasonal Thermal Energy Storage, methodology, architecture

1. Introduction

Fuel price inflation, a long-term increase in power consumption, and related to them CO_2 emissions [1, 2] have provided added impetus to the search for ultra-effective heat and power generation systems [3–5]. Space heating and hot water production consume more than one third of the primary energy in industrialized countries like Poland. Set against this backdrop, the researchers investigated solar thermal technology as a means of significantly enhancing the conservation of fossil fuels and reduction of emissions. In the case of electricity generation, solar energy can be used indirectly by utilizing biofuels, the most promising technology being fuel cells which generate power in electrochemical reactions with potentially ultra-high efficiency [6–15].

Hot-water production by solar energy has become a competitive solution [16], but the use of solar radiation in domestic heating has been minimal in countries such as Poland—thermal energy from the sun for heating is only possible on a seasonal basis. The energy density of solar radiation is low, and radiation is at its maximum in summer whereas heat is mainly needed in winter. Therefore, seasonal heat storage is necessary if more than about 20% of the heat demand is to be met by solar energy. There are many means of storing seasonal thermal energy.

The problem of seasonal thermal energy storage in the ground was raised in [17], which analyzed the impact of selected parameters on heat storage capacity, such as ground moisture adjacent to the energy store. Calculations were made for heat and water movement—but assumed the level of storage to be up to 90°C. Based on the data model, a pilot plant was designed based on waste heat of 174 kW_{th}. The heat reservoir had a capacity of 15,000 m^3 and consisted of 140 vertical heat exchangers with a depth of 30 m. A preliminary analysis of the cost of building the system was presented. The storage of thermal energy in rock was proposed in [18]. Based on mathematical modeling, an estimation was presented of speci-

*Corresponding author
Email addresses: milewski@itc.pw.edu.pl (Jarosław Milewski*), mwolo@itc.pw.edu.pl (Marcin Wolowicz), bujalski@itc.pw.edu.pl (Wojciech Bujalski)

fied storage capacities of rock in early preparation for heat loss of 10...20% during one cycle. The size of the storage facility was taken in the range 50...250 m depth, with the medium being propane. The computational models presented in [19–23] were used to determine the long term performance of a spherical/hemispherical thermal energy storage vessel for both heating and cooling purposes. They showed that a collector area greater than 60 m^2/house does not yield a significant advantage for the climatic conditions of Turkey. The authors repeated their calculations for cylindrical storage in [24], in which they present a slightly higher solar fraction of the design. The optimum integration of condensing boilers, compression and absorption heat pumps, and cogeneration of heat and power computed for 100 well-insulated housing units is presented in [25]. Compared with a reference case with individual condensing boilers and electricity taken from the public grid, selected scenarios achieve energy savings associated with cost increases. They obtained a solar contribution to the heat supply of 80%, which translates into fossil fuel savings of more than 40% if electricity is produced from non-fossil energy sources. [26] presents simulations of a solar heating system for 90 buildings of 100 m^2 floorspace each. It was shown that 3,000 m^2 of roof-mounted solar collectors and a borehole storage system (60,000 m^3) would satisfy 60% of the total heat demand. In [27], a central solar heating plant with seasonal ground storage is analyzed through dynamic system simulations. A system such as this is intended to use solar energy to satisfy 50% of the heat demand. Apart from global indicators (e.g. solar fraction), it is necessary to simulate transient behavior of the system. Determining an adequate control strategy is a very important task and can be realized by classic algorithms as well as artificial intelligence tools (as was proved in other fields e.g. [28–32]). Some improvements to system control are also investigated to assess the influence on the overall thermal performances of the system. In [33], thermal performance and economic feasibility of three types of solar central heating systems with seasonal storage in Turkey are investigated and the researchers concluded that a minimum payback period of 19 years, increasing to 40 years if a 100% solar fraction is achieved [34]. Publication [35] contains the results of simulations of a large seasonal heat storage facility in China. The installation consists of 1,000 m^2 of solar panels and an underground heat storage tank with a capacity of 90,000 m^3. The study involved a relatively low temperature: 30°C. A good overview of the technologies used for seasonal storage of thermal energy is included in the publication [36]—where all the possibilities discussed here occur—even the very exotic. The simulation results in long-term futures (5 years) included in the publication [37]. It uses commercially available software (TRNSYS—the most popular software for calculating STES dynamic behavior, inter alia [38, 39]), to determine the operating parameters of systems of this type, while other software is used, and reported, to compute a transient operation [40].

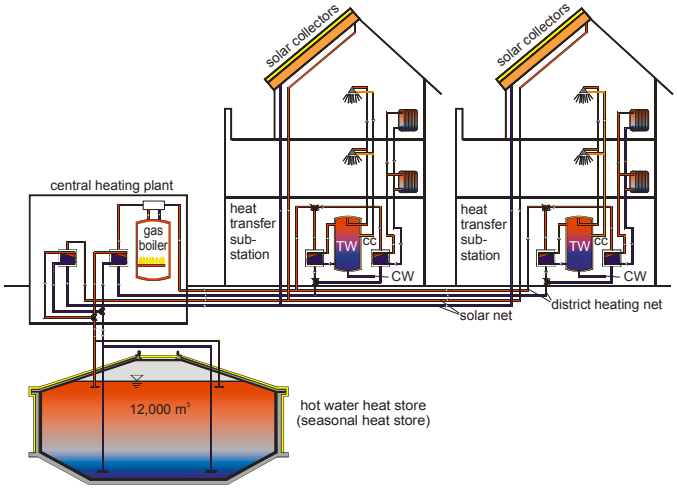

Figure 1: The idea of STES [41]

Conditions associated with solving optimization tasks arise from cooperation under the agreement: thermal storage tank + band devices + heat source + district heating. District heating (load) is characterized by variability of demand, depending on the season (heating season, transitional periods, summer season), weekdays (working days period before, during and after the weekend), and finally the time of day. The manufacturer uses in addition a heat and electricity co-generation plant to satisfy conditions resulting from the specific electricity market (contracts for the supply of electricity often involve more than one recipient, an emphasis on delivery in accordance with established graphic loads and the ability to use active participation in the energy market, e.g.,

power exchange to restrict the sale/purchase on the balancing market, the possibility to use variables in a day for electricity prices to maximize profits from electricity sales—this last opportunity to meet national conditions with the appropriate tariff adjustment.) The possibility of cooperation using a thermal storage tank combined with a source of heat and electricity determines the currently available configuration (variable in time) of working devices and their design features.

The indicated conditions and design features of the system result in the thermal storage tank causing significant setback restrictions in formulating the process model and the optimization task.

Certain assumptions are made for the development of the specified heating system and connection with the energy source (one source): a set of typical situations for combining thermal storage tank operation with the network, activities in typical situations, and in a given time horizon. We sought to identify ways of optimizing operation using the source thermal storage tank, we developed an algorithm and test methods to optimize the selected scenarios, identified potential effects of optimization of the thermal storage tank and, finally, attempted to generalize the results to conditions typical for national geographic and weather conditions.

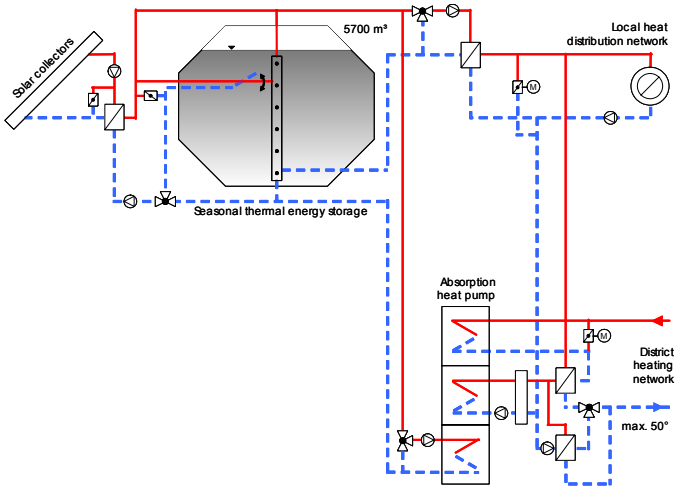

Figure 2: System concept of the solar assisted district heating system in Munich [42]

Specific conditions are highly relevant to optimizing the operating parameters of a heating network including a heat reservoir. In many countries (notably Denmark, Germany and Sweden) there are numerous combinations of heating systems, heat storage tanks, including some which are very large. For those very diverse networks methods of treatment have been developed to achieve the most efficient use of thermal storage tanks so as to increase operational efficiency (in economic terms) of the energy source. Procedures have been put in place to thermal storage tanks to compensate for peak loads, and to work in tandem for longer periods.

It is difficult to develop a rational way of using the thermal storage tank solely on the basis of the experience and intuition of the operators. The decision to top-up or unload is affected by a number of key factors, including: forecast load (related to the weather forecast), the current state of the network (dynamic changes in temperature and flow—current and projected), the current state of the heat source (which devices are in operation, the status of their loads, technological capabilities and effectiveness of changes, inclusions or exclusions.) For these issues there is no experience in the application of optimization methods, especially taking into account the dynamics of changes in economic conditions (changing regulations and prices.) For this type of problem modern approaches are needed that take into account adaptation to changing conditions, although insufficient recognition has been given thus far to applying them to issues of long-term optimization of thermal storage tanks. The problem of co-operation of district heating thermal storage tanks is the subject of the work carried out by a few national centers, mainly Silesian University of Technology (prof. Ziebik et al. [44–49], prof. Skorek et al. [50–52]) and Warsaw University of Technology (prof. Mankowski et al. [53, 54] and the application works carried out on request of industry). Works of prof. Skorek et al. relate primarily to applications for small district heating systems. Works of dr. Zuwala and prof. Ziebik were oriented largely to the question of optimal size of the thermal storage tank. The problem of efficiency (optimization) service thermal storage tanks in the field selected from the complex aspects of the complex appeared in the work of dr. Zuwala.

There are a few types of STES:

- Tank thermal energy storage (TTES):

Table 1: Seasonal thermal energy storage in Germany [43]

Location	Type	Size, m^3	Start oi operation
Rottweil	hot-water (concrete)	600	1995
Friedrichshafen	hot-water (concrete)	12,000	1996
Hamburg	hot-water (concrete)	4,500	1996
llmenau	hot-water (GRP)	300	1997/1998
Hanover	hot-water (HOC)	2,750	2000
Munich	hot-water (concrete)	5,700	2007
Stuttgart	gravel/water	1,060	1984
Chemnitz	gravel/water	8,000	1995/2000
Augsburg	gravel/water	6,500	1997
Steinfurt	gravel/water	1,500	1999
Eggenstein	gravel/water	4,600	2008
Neckarsulm	BTES	63,360	1997+1998+2001
Crallshelm	BTES	35,700	2008
Berlin	ATES	n/a	1999
Rostock	ATES	20,000	2000
Neubranden-burg	ATES	n/a	2004
Attenkirchen	hot-water/BTES	9,860	2002

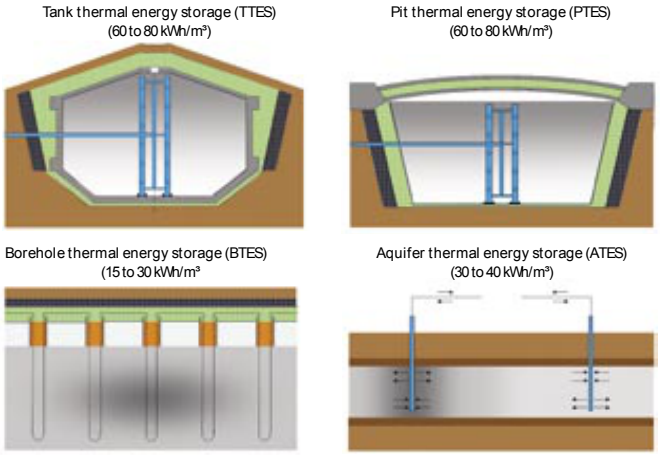

Figure 3: The four technologies for storing solar thermal energy seasonally [55]

60...80 kWh/m^3

- Pit thermal energy storage (PTES): 60...80 kWh/m^3 [56]
- Borehole thermal energy storage (BTES): 15...30 kWh/m^3 [26, 57, 58]
- Aquifer thermal energy storage (ATES): 30...40 kWh/m^3 [59, 60]
- Thermochemical energy storage: 140...460 kWh/m^3 [61–64]
- Phase Change Material storage (PCM) [65]

The typical operating temperature of a STES is in the range 70/35°C. An additional advantage is given by proper operation of the STES to maintain stratification inside the tank. Good stratification results in 20...40% higher efficiency and enables the network to be fed by constant inlet and outlet water temperatures. On the other hand, thermocline expands during normal operation. Based on a review of the literature, a typical ratio of tank volume to solar panel area (V/A ratio) is about 2 m (m^3/m^2) [25].

In many cases, a local heat storage facility in Polish conditions will probably work with the local heat supplier—urban heating system—which is supplied by coal fired Combined Heat and Power (CHP) plants [66], which will be characterized by local circumstances that are substantially different to the typical characteristics of known determinants from experience elsewhere. For this reason, the economic conditions of work of these thermal storage tanks and pre-defined scenarios of work cannot be transferred directly to the Polish environment. Our previous paper [67] demonstrates a reliable solar hearing system with seasonal storage at an already existing and poorly thermally-insulated complex of buildings. The aim of this preliminary study was to find a suitable system design with low energy cost at a solar fraction of about 60% or above and to compare the size of the storage with the buildings. While the tank volume is chosen at an arbitrary value, we analyze the influence of the chosen architecture parameters of the tank to demonstrate their influence on the thermal capacity of the storage facility. The presented results were obtained by dynamic modeling of the system using software [68].

2. Theory

This section presents the basic factors for judging STES systems. It is necessary to use absolute heat amounts (not heat flux) for the purpose of analyzing the quality of energy conversion in the STES system, because of the different periods of consumption and supply of heat to the customer and various heat flux values. The process parameters are variable in time, e.g., heat capacity can be time-dependent as can be

the accumulator feeding temperature (if it is variable). Process management and the conditions inside the reservoir affect the timing and regime for charging and discharging the accumulator. An appropriate dynamic model of the plant needs to be constructed for the purpose of determining those regimes.

A comparison of different STES plant variants can be done using the following factors. There are two definitions which can be used to judge the amount of energy stored:

$$\eta_{\mathrm{I}} = \frac{Q_{heating}}{Q_{solar}} \tag{1}$$

$$\eta_{\mathrm{II}} = \frac{Q_{heating}}{Q_{Sun}} \tag{2}$$

where: $Q_{heating}$—amount of heat delivered by a STES; Q_{solar}—amount of heat delivered by solar panels; Q_{Sun}—theoretical value of heat provided by the sun.

The first regards heat delivered by STES to the customer in relation to heat delivered by the solar collectors. On average, 50...70% of the stored heat can be utilized during the heating season. The second definition takes into account total energy given by the sun, and is usually in the region of 6%.

The effectiveness of the way heat is stored in a STES can be expressed by the Cycle Number (CN) factor as:

$$CN = \frac{Q_{heating}}{Q_{stored}} \tag{3}$$

where: Q_{stored}—amount of heat stored in a STES.

Usually, the CN factor is kept in or around 1.5. The amount of heat stored in a STES can be estimated using the following relationship:

$$Q_{stored} = V_{store} \cdot \rho_{water} \cdot c_{water} \cdot (T_{\max} - T_{\min}) \tag{4}$$

where: V_{store}—volume of a STES, ρ—density, c—heat capacity, T—temperature.

An additional factor called "solar fraction" also describes the operating efficiency of the system and is defined by the following function:

$$\eta = \frac{Q_{solar}}{Q_{heating}} \tag{5}$$

Based on the previously indicated values, the solar fraction is around 30%.

$$\eta_{STES} = \frac{Q_{heating}}{E_{elc} \cdot COP + Q_f + Q_{solar}} \tag{6}$$

where: E_{elc}—electricity delivered to a heat pump, Q_f—chemical energy delivered to an auxiliary boiler

It is not always convenient to use the efficiency definition 1 because it requires adding up two different kinds of energy: electricity delivered by the grid for the heat pump and chemical energy supplied with the fuel. From this point of view it would be more appropriate to use the equation 6, which includes the efficiency of heat generation by a heat pump and additional boiler. This method is an attempt to evaluate the consumption of the fuel energy required to generate all the heat delivered by the STES plant.

In order to avoid having to add up different kinds of energy (heat, electricity and chemical energy), the efficiency of a STES plant can also be defined as:

$$\eta_{STESf} = \frac{Q_{heating} - Q_{stored}}{Q_f + E_{elc} \cdot COP} \tag{7}$$

considering the STES technological process as a form of heat generation based on delivered fuel. Efficiency defined in this way describes the effectiveness of fuel consumption in the generation of net heat output of the plant. It has to be emphasized that the equation 7 can result in a negative result (when $Q_{stored} > Q_{heating}$) or infinity (if $Q_f + E_{elc} \cdot COP = 0$).

The energy density of solar insolation is low (about 130 W/m^2 annual average in southern Poland), and insolation reaches its zenith in summer. Heat delivered by solar panels depends on several factors (time of day, season, cloud cover etc.), on average a solar panel in southern Poland can deliver about 200...600 kW/m^2/a. Based on data collected for other STESes, the average heat delivered by solar panels is assumed at 300 kW/m^2/a.

2.1. Tank

The heat flow is calculated as follows:

$$\dot{Q} = U \cdot A \cdot (T_{Amb} - T)$$

where: $\dot{Q}$—heat flow, U—the overall heat transfer coefficient; A—the heat transfer area; T_{Amb}—the ambient temperature; T—holdup temperature.

Heat Flow is defined as the heat flowing into the vessel. The heat transfer area is calculated from the vessel geometry.

The steady-state mode vessel energy balance is defined below:

$$\dot{Q}_{feed} \pm \dot{Q}_{duty} = \dot{m}_{vapour} \cdot h_{vapour} + \dot{m}_{heavy} \cdot h_{heavy} + \dot{m}_{light} \cdot h_{light}$$

where: $\dot{Q}_{feed}$—heat flow of the feed streams, $\dot{m}$—mass flow, h—enthaply.

The amount of liquid volume, or holdup, in the vessel at any time is given by the following expression:

$$V_{holdup} = V_{vesel} \cdot \frac{l_{liquid,full}}{100}$$

where: $l_{liquid,full}$— liquid level in the vessel at time t.

2.2. Pump

For the pump, calculations are based on the standard pump equation for power, which uses the pressure rise, the liquid flow rate and density.

$$P_{pump,ideal} = \frac{(p_{out} - p_{in}) \cdot \dot{v}}{\rho_{liquid}}$$

where: p_{out}—pump outlet pressure, p_{in}—pump inlet pressure, $\dot{v}$—flow rate.

The above equation defines the ideal power needed to raise the liquid pressure. The actual power requirement of the pump is defined in terms of the pump's efficiency.

$$\eta_{pump} = \frac{P_{pump,ideal}}{P_{pump}}$$

When efficiency is less than 100%, the excess energy goes into raising the temperature of the outlet stream.

Combining the above equations leads to the following expression for the actual power requirement of the pump:

$$P_{pump} = \frac{(p_{out} - p_{in}) \cdot \dot{v}}{\rho_{liquid} \cdot \eta_{pump}}$$

Finally, the actual power is equal to the difference in heat flow between the outlet and inlet streams:

$$P_{pump} = \dot{m} \cdot (h_{out} - h_{in})$$

The rate of energy required to accelerate the speed of a pump is a function of the rotational inertia of the impeller and the rotational speed: The rotational inertia, I, is calculated as follows:

$$I = M \cdot r^2$$

where: M—the mass of the impeller and rotating shaft, r—the radius of gyration.

The rate of energy required to accelerate the impeller, E_1, can be calculated using:

$$E_1 = I \cdot |\omega| \cdot \frac{d\omega}{dt}$$

where: ω—the rotation speed.

The rate of energy lost from mechanical inefficiencies depends on the frictional power loss factor, f_{fric}:

$$E_f = f_{fric} \cdot \omega |\omega|$$

Typical values for f_{fric} should be around 0.0001.

2.3. Heater/Heat exchanger

The enthalpy or heat flow of the energy stream is added to the heater's process side holdup:

$$\dot{m} \cdot (h_{in} - h_{out}) + \dot{Q}_{heater} = \frac{d\,(V h_{out})}{dt}$$

where: $\dot{m}$—process fluid flow rate, h—enthalpy, $\dot{Q}_{heater}$—heater duty, V—volume shell or tube holdup.

The k value is used to relate the frictional pressure loss and flow through the heater. This relation is similar to the general valve equation:

$$\dot{m} = \sqrt{\rho} \cdot k \cdot \sqrt{p_1 - p_2}$$

This general flow equation uses the pressure drop across the heat exchanger without any static head contributions. The quantity, $p_1 - p_2$, is defined as the frictional pressure loss which is used to "size" the heater with a k-value.

The heat exchanger calculations are based on energy balances for the hot and cold fluids. The following general relation applies to the shell side of the basic model of the heat exchanger:

$$\dot{m}_{shell} \cdot (h_{in} - h_{out})_{shell} - \dot{Q} = \frac{d\,(Vh_{out})_{shell}}{dt}$$

For the tube side:

$$\dot{m}_{tube} \cdot (h_{in} - h_{out})_{tube} - \dot{Q} = \frac{d\,(Vh_{out})_{tube}}{dt}$$

where: $\dot{m}_{shell}$—shell fluid flow rate, $\dot{m}_{tube}$—tube fluid flow rate, h—enthalpy, $\dot{Q}_{loss}$—heat loss, $\dot{Q}$—heat transfer from the tube side to the shell side, V—volume shell or tube holdup.

The term $\dot{Q}_{loss}$ represents the heat lost from the shell side of the dynamic heat exchanger.

The total heat transferred between the tube and shell sides (heat exchanger duty) may be defined in terms of the overall heat transfer coefficient, the area available for heat exchange and the log mean temperature difference:

$$\dot{Q} = U \cdot A \cdot \triangle T_{LM} \cdot F_t$$

where: U—overall heat transfer coefficient, A—surface area available for heat transfer, $\triangle T_{LM}$—Log mean temperature difference (LMTD), F_t—LMTD correction factor.

The heat transfer coefficient and the surface area are often combined for convenience into a single variable referred to as UA.

For fluids without phase change, the local heat transfer coefficient, k_i, is calculated according to the Sieder-Tate correlation:

$$k_i = \frac{0.023 D_i}{k_m} \left(\frac{D_i G_i}{\mu_i}\right)^{0.8} \left(\frac{C_{p,i}\mu_i}{k_m}\right)^{\frac{1}{3}} \left(\frac{\mu_i}{\mu_{i,w}}\right)^{0.14}$$

where: G_i—Mass velocity of the fluid in the tubes (velocity×density), μ_i—Viscosity of the fluid in the tube (at bulk temperature), $\mu_{i,w}$—Viscosity of the fluid inside tubes, at the tube wall, $C_{p,i}$—Specific heat capacity of the fluid inside the tube.

The relationship between the local heat transfer coefficients and the overall heat transfer coefficient is:

$$U = \frac{1}{\left[\frac{1}{k_o} + r_o + r_w + \frac{D_o}{D_i}\left(r_i + \frac{1}{k_i}\right)\right]}$$

where: U—overall heat transfer coefficient, k_o—local heat transfer coefficient outside tube, k_i—local heat transfer coefficient inside tube, r_o—fouling factor outside tube, r_i—fouling factor inside tube, r_w—tube wall resistance, D_o—outside diameter of tube, D_i—inside diameter of tube.

2.4. PID (Proportional-Integral-Derivative) Controller

Process Variable (PV) is the measured variable which the controller is trying to keep at the Set Point (SP). The following equation is used to translate a PV value into a percentage of the range:

$$PV = \left(\frac{PV - PV_{\min}}{PV_{\max} - PV_{\min}}\right)$$

The OP (or Output) is the percentage opening of the control valve. The Controller manipulates the valve opening for the Output Stream in order to reach the set point.

The characteristic equation for a PID Controller is given below:

$$OP\,(t) = OP_{ss} + K_p E\,(t) + \frac{K_p}{T_i}\int E\,(t) + K_p T_d \frac{dE\,(t)}{dt}$$

where: $OP\,(t)$—Controller output at time t, OP_{ss}—Steady-State controller output (at zero error), $E\,(t)$—Error at time t, K_p—Proportional gain of the controller, T_i—Integral (reset) time of the controller, T_d—Derivative (rate) time of the controller.

The error at any time is the difference between the Set Point and the Process Variable:

$$E\,(t) = SP\,(t) - PV\,(t)$$

The PID (Proportional-Integral-Derivative) Controller requires values for all three of K_p, T_i and T_d.

The ATV (Auto Tune Variation) Technique is one of a number of techniques used to determine two important system constants known as the Ultimate Period, and the Ultimate Gain. From these constants, tuning values for proportional, integral, and derivative gains can be determined.

The Ultimate Gain can be calculated from the following relationship:

$$KU = \frac{4h}{\pi a}$$

where: KU—Ultimate Gain, h—Change in OP (0.05), a —Amplitude.

The Controller Gain and Integral Time can be calculated as follows:

$$Controller\,Gain = KU/3.2$$

$$Controller\,Integral\,Time = 2.2 \cdot PU$$

3. Choosing the STES architecture—methodology

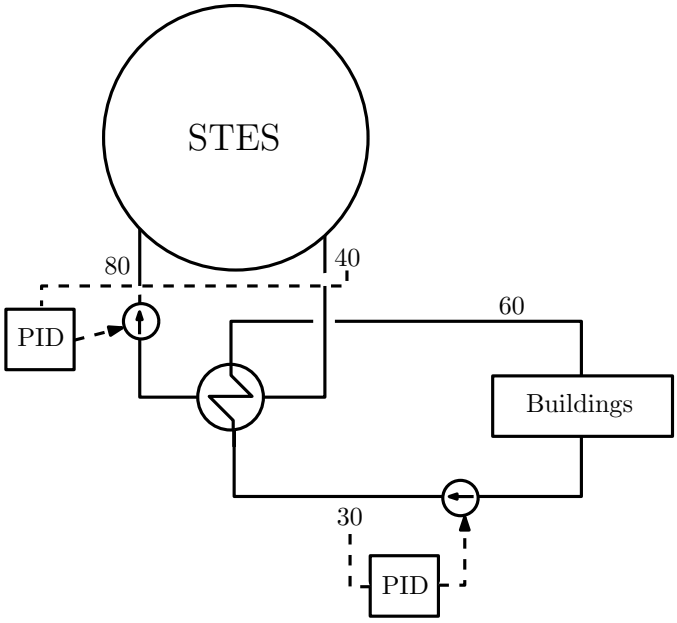

Figure 4: Temperatures and PID controllers in STES/buildings connection

The analyzed system is composed of the tank, solar panels and building—see Fig. 4. All those elements are connected by two independent networks. The solar panels are mounted on the building's roof and are used for heating the building, so only excess heat can be directed to the heat storage facility. Two heating networks are connected to each other by a heat exchanger, and water flow (tank loading flow) is controlled by PID (to keep the set temperature of loading).

Table 2: Assumptions for model construction

Parameter	Value	Comment
Tank diameter, m	30	
Tank height, m	4.4	
Tank volume, m^3	3,000	
Water volume, m^3	2,800	90% of the tank volume
Charging temperature, °C	80	
Heat transfer coefficient, U, kJ/h/m^2/°C	0.4824	granulated glass
Specific thermal conductivity: λ, W/m/K	0.094	
Total thermal conductivity: λ/δ, W/m^2/K	0.4824	
Insulation thickness, cm	70	
Solar collectors area, m^2	2,000	
Annual average sun heat rate, kWh/m^2/a	300	

Table 3: Solar heat, kW

Month	Solar panels	Buildings heat consumption	Difference	Charging
January	24.70	516.04	491.34	0.00
February	27.38	450.19	422.81	0.00
March	49.19	453.29	404.10	0.00
April	63.44	396.22	332.78	0.00
May	87.28	186.90	99.61	0.00
June	92.11	49.70	-42.41	42.41
July	92.76	46.34	-46.42	46.42
August	83.97	39.40	-44.57	44.57
September	55.50	51.78	-3.72	3.72
October	35.06	78.16	43.10	0.00
November	16.64	292.68	276.04	0.00
December	13.66	347.72	334.06	0.00

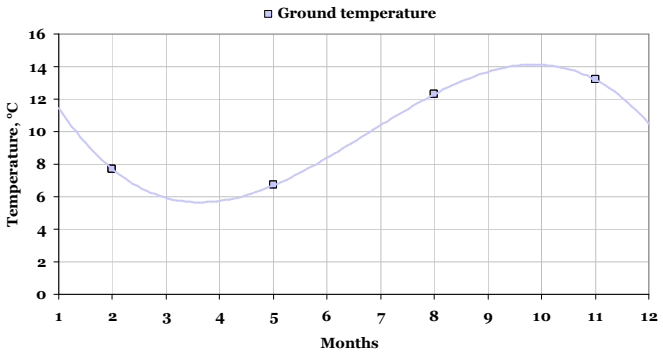

Figure 5: Ground temperature depends on month

The main parameters of the reference case and assumptions made during model construction are presented in Table 2.

All but case of the analyzed cases consider a tank

placed in the ground, with the ground temperature assumed to vary during the year as shown in Fig. 5.

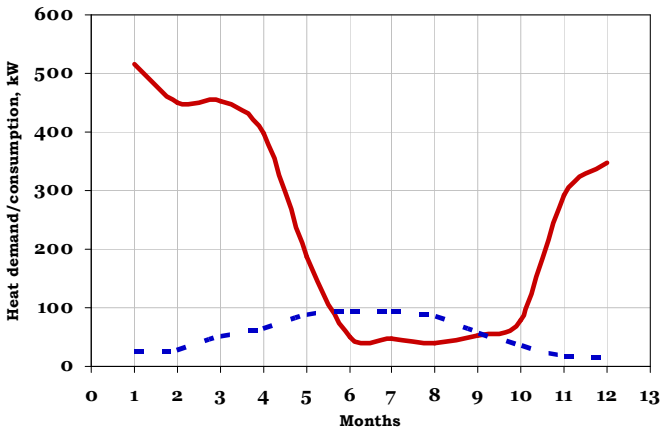

Figure 6: Heat demand of the buildings and adequate solar thermal energy, kW

The heat generated by the solar panels and demanded by the buildings is shown in Fig. 6. Based on the data shown, solar heat can be stored up in the period from June to September, later on the heat can be utilized or stored for use in other months. The analysis considers only the heat losses during the winter season to define the amount of thermal energy available during the heating season.

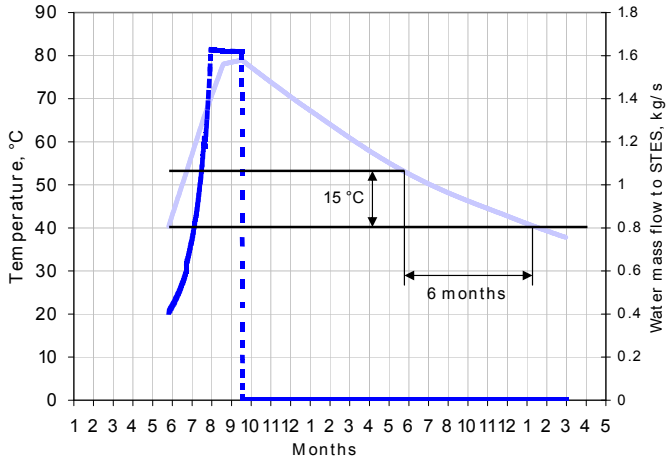

Figure 7: Results based on calculations including presented assumptions

The results obtained for the reference case are shown in Fig. 7. The heat storage facility is fully charged in September and then the water temperature falls due to heat losses into the surroundings (the ground). Water temperature at the beginning of the following June is about 15°C above the initial temperature. Thus, the available thermal energy storage in the tank is 175 GJ (67.5 kW·month). Hence, heat storage effectiveness is about 38%, for non-optimal tank architecture (height/diameter, h/d = 0.15), whereas the optimal dimensions of the tank should be around h/d = 1). During this simulation there is no stratification assumed—in real conditions stratification strongly depends on the height of the tank, thus the optimal dimensions can be varied from the assumed h/d = 1.

Four other cases were taken into consideration:

1. Case 1—short tank with a height of 2 m (h/d = 0.05)
2. Case 2—tall tank with a height of 8 m (h/d = 0.42)
3. Case 3— very tall tank with a height of 16 m (h/d = 1.17)
4. Case 4—very tall tank owith a height of 16 m (h/d = 1.17) located outside (not in the ground)

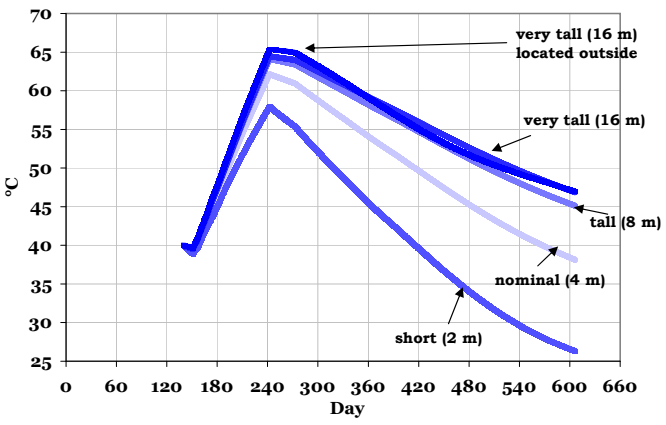

Figure 8: Results of the sensitivity analysis of the influence of tank geometry parameters on thermal storage capacity

4. Discussion and conclusions

The preliminary study for a STES system is shown for Polish conditions. The analysis was carried out for five different scenarios for various tank dimensions and locations. The results are compared against the chosen nominal point (4 m tank height located in the ground). The available thermal energy shown by

heat losses to the surroundings is about 62.5 MJ/m^3 at the nominal point, which gives 15°C of water temperature for use with an effectiveness factor of 38%. By changing the tank geometries, the available thermal energy can be raised to 83 MJ/m^3 (effectiveness of 50%).

There is almost no difference if the tank is located in the ground or outside—lower ground temperatures in summer results in higher thermal losses which are compensated during the winter when higher thermal losses are recorded for the tank located outside. One significant advantage for placing the tank in the ground is when the tank is fully discharged during winter—no danger of freezing.

During spring/autumn relatively low thermal power is needed for discharging, thus an existing natural gas boiler can be started up later and shut down earlier. The following control strategies for STES operation can be stated:

1. To meet the heat demand of ta standalone building
   (a) immediately start with the heating season
   (b) relatively low heat flux during discharging
2. Monitoring natural gas prices
   (a) existing NG boilers charge the STES during periods of low fuel prices
   (b) difficulties in price forecasting
3. Rapid discharge
   (a) minimal heat losses
   (b) danger of freezing if the tank is located outside

Acknowledgments

The project was funded by the National Science Center allocated on the basis of decision number DEC-2012/07/B/ST8/03937.

References

[1] W. Budzianowski, Modelling of co2 content in the atmosphere until 2300: Influence of energy intensity of gross domestic product and carbon intensity of energy, International Journal of Global Warming 5 (1) (2013) 1–17.

[2] J.-H. Wee, Carbon dioxide emission reduction using molten carbonate fuel cell systems, Renewable and Sustainable Energy Reviews 32 (2014) 178–191.

[3] L. Bartela, J. Kotowicz, Analysis of operation of the gas turbine in a poligeneration combined cycle, Archives of Thermodynamics 34 (4) (2013) 137–159.

[4] T. Bartela, A. Skorek-Osikowska, J. Kotowicz, Economic analysis of a supercritical coal-fired chp plant integrated with an absorption carbon capture installation, Energy 64 (2014) 513–523.

[5] Łukasz Nikonowicz, J. Milewski, Determination of electronic conductance of solid oxide fuel cells, Journal of Power Technologies 91 (2) (2011) 82–92.

[6] D. Bakalis, A. Stamatis, Incorporating available micro gas turbines and fuel cell: Matching considerations and performance evaluation, Applied Energy 103 (2013) 607–617.

[7] R. Chacartegui, B. Monje, D. Sánchez, J. Becerra, S. Campanari, Molten carbonate fuel cell: Towards negative emissions in wastewater treatment chp plants, International Journal of Greenhouse Gas Control 19 (2013) 453–461.

[8] C. Guerra, A. Lanzini, P. Leone, M. Santarelli, D. Beretta, Experimental study of dry reforming of biogas in a tubular anode-supported solid oxide fuel cell, International Journal of Hydrogen Energy 38 (25) (2013) 10559–10566.

[9] E. Jannelli, M. Minutillo, A. Perna, Analyzing microcogeneration systems based on lt-pemfc and ht-pemfc by energy balances, Applied Energy 108 (2013) 82–91.

[10] D. McLarty, J. Brouwer, S. Samuelsen, Hybrid fuel cell gas turbine system design and optimization, Journal of Fuel Cell Science and Technology 10 (4).

[11] J. Qian, Z. Tao, J. Xiao, G. Jiang, W. Liu, Performance improvement of ceria-based solid oxide fuel cells with yttria-stabilized zirconia as an electronic blocking layer by pulsed laser deposition, International Journal of Hydrogen Energy 38 (5) (2013) 2407–2412.

[12] S. Sieniutycz, J. Jezowski, Energy Optimization in Process Systems and Fuel Cells, 2013.

[13] J. Stempien, Q. Sun, S. Chan, Performance of power generation extension system based on solid-oxide electrolyzer cells under various design conditions, Energy 55 (2013) 647–657.

[14] S.-B. Wang, C.-F. Wu, S.-F. Liu, P. Yuan, Performance optimization and selection of operating parameters for a solid oxide fuel cell stack, Journal of Fuel Cell Science and Technology 10 (5).

[15] W. Wang, H. Li, X.-F. Wang, Analyses of part-load control modes and their performance of a sofc/mgt hybrid power system, Dalian Ligong Daxue Xuebao/Journal of Dalian University of Technology 53 (5) (2013) 653–658.

[16] F. Chabane, N. Moummi, S. Benramache, Experimental analysis on thermal performance of a solar air collector with longitudinal fins in a region of biskra, algeria, Journal of Power Technologies 93 (1) (2013) 52–58.

[17] M. Reuss, M. Beck, J. Müller, Design of a seasonal thermal energy storage in the ground, Solar energy 59 (4) (1997) 247–257.

[18] G. Hellström, S. Larson, Seasonal thermal energy

storage–the hydrock concept, Bulletin of Engineering Geology and the Environment 60 (2) (2001) 145–156.
[19] M. Inalli, M. Unsal, V. Tanyildizi, A computational model of a domestic solar heating system with underground spherical thermal storage, Energy 22 (12) (1997) 1163–1172.
[20] R. Yumrutaş, M. Ünsal, A computational model of a heat pump system with a hemispherical surface tank as the ground heat source, Energy 25 (4) (2000) 371–388.
[21] R. Yumrutaş, M. Ünsal, Analysis of solar aided heat pump systems with seasonal thermal energy storage in surface tanks, Energy 25 (12) (2000) 1231–1243.
[22] R. Yumrutaş, M. Kanoğlu, A. Bolatturk, M. Ş. Bedir, Computational model for a ground coupled space cooling system with an underground energy storage tank, Energy and buildings 37 (4) (2005) 353–360.
[23] R. Yumrutaş, M. Ünsal, Modeling of a space cooling system with underground storage, Applied thermal engineering 25 (2) (2005) 227–239.
[24] M. Inalli, Design parameters for a solar heating system with an underground cylindrical tank, Energy 23 (12) (1998) 1015–1027.
[25] D. Lindenberger, T. Bruckner, H.-M. Groscurth, R. Kümmel, Optimization of solar district heating systems: seasonal storage, heat pumps, and cogeneration, Energy 25 (7) (2000) 591–608.
[26] B. Nordell, G. Hellström, High temperature solar heated seasonal storage system for low temperature heating of buildings, Solar Energy 69 (6) (2000) 511–523.
[27] D. Pahud, Central solar heating plants with seasonal duct storage and short-term water storage: design guidelines obtained by dynamic system simulations, Solar Energy 69 (6) (2000) 495–509.
[28] M. Amirinejad, N. Tavajohi-Hasankiadeh, S. Madaeni, M. Navarra, E. Rafiee, B. Scrosati, Adaptive neuro-fuzzy inference system and artificial neural network modeling of proton exchange membrane fuel cells based on nanocomposite and recast nafion membranes, International Journal of Energy Research 37 (4) (2013) 347–357.
[29] S. Hajimolana, S. Tonekabonimoghadam, M. Hussain, M. Chakrabarti, N. Jayakumar, M. Hashim, Thermal stress management of a solid oxide fuel cell using neural network predictive control, Energy 62 (2013) 320–329.
[30] D. Marra, M. Sorrentino, C. Pianese, B. Iwanschitz, A neural network estimator of solid oxide fuel cell performance for on-field diagnostics and prognostics applications, Journal of Power Sources 241 (2013) 320–329.
[31] O. Razbani, M. Assadi, Artificial neural network model of a short stack solid oxide fuel cell based on experimental data, Journal of Power Sources 246 (2014) 581–586.
[32] A. Zamaniyan, F. Joda, A. Behroozsarand, H. Ebrahimi, Application of artificial neural networks (ann) for modeling of industrial hydrogen plant, International Journal of Hydrogen Energy 38 (15) (2013) 6289–6297.
[33] A. Ucar, M. Inalli, Thermal and economic comparisons of solar heating systems with seasonal storage used in building heating, Renewable Energy 33 (12) (2008) 2532–2539.
[34] A. Simons, S. K. Firth, Life-cycle assessment of a 100% solar fraction thermal supply to a european apartment building using water-based sensible heat storage, Energy and Buildings 43 (6) (2011) 1231–1240.
[35] J. Zhao, Y. Chen, S. Lu, Simulation study on operating modes of seasonal underground thermal energy storage, in: Proceedings of ISES World Congress 2007 (Vol. I–Vol. V), Springer, 2009, pp. 2119–2122.
[36] P. Pinel, C. Cruickshank, I. Beausoleil-Morrison, A. Wills, A review of available methods for seasonal storage of solar thermal energy in residential applications, Renewable and Sustainable Energy Reviews 15 (7) (2011) 3341–3359.
[37] M. Sweet, J. McLeskey, Numerical simulation of underground seasonal solar thermal energy storage (sstes) for a single family dwelling using trnsys, Solar Energy.
[38] M. de Guadalfajara, M. A. Lozano, L. M. Serra, Evaluation of the potential of large solar heating plants in spain, Energy Procedia 30 (2012) 839–848.
[39] M. L. Sweet, J. T. McLeskey Jr, Numerical simulation of underground seasonal solar thermal energy storage (SSTES) for a single family dwelling using TRNSYS, Solar Energy 86 (1) (2012) 289–300.
[40] K. Çomaklı, U. Çakır, M. Kaya, K. Bakirci, The relation of collector and storage tank size in solar heating systems, Energy Conversion and Management 63 (2012) 112–117.
[41] T. Schmidt, J. Nussbicker, Monitoring results from german central solar heating plants with seasonal storage, in: Solar World Congress, ISES, 2005, pp. 1–6.
[42] T. Schmidt, D. Mangold, New steps in seasonal thermal energy storage in germany, Tech. rep., Solites - Steinbeis Research Institute for Solar and Sustainable Thermal Energy Systems (2006).
[43] T. Schmidt, Seasonal thermal energy storage - pilot projects and experiences in germany, Tech. rep., Steinbeis Research Institute for Solar and Sustainable Thermal Energy Systems (2008).
[44] A. Ziębik, J. Zuwała, Analiza techniczno-ekonomiczna zastosowania zasobnika ciepła w elektrociepłowni z turbiną przeciwprężną w celu maksymalizacji produkcji szczytowej energii elektrycznej, Gospodarka Paliwami i Energią (2) (2000) 8–12.
[45] A. Ziębik, J. Zuwała, C. CIASNOCHA, Dobór optymalnej wielkoœci zasobnika ciepła przy zadanym wykresie rzeczywistym obciążeń w elektrociepłowni z turbiną przeciwprężną, Energetyka (9) (2001) 507–517.
[46] J. Zuwała, Korzyści energetyczne i ekonomiczne zastosowania zasobników ciepła w elektrociepłowniach, Gospodarka Paliwami i Energią (5-6) (2002) 17–21.
[47] J. Zuwała, Dobór optymalnej mocy turbiny i zasobnika ciepła dla elektrociepłowni z turbiną przeciwprężną, Archiwum Energetyki 34 (2 s 185).
[48] A. Ziębik, A. Fręchowicz, J. Zuwała, Analiza porównawcza jednoprzewodowego systemu przesyłania ciepła

z zastosowaniem zasobników ciepła, Prace Naukowe Politechniki Warszawskiej. Mechanika (211) (2005) 319–330.

[49] J. Zuwała, Wpływ" trybu weekendowego" pracy zasobnika ciepła na strukturę wytwarzania energii elektrycznej w elektrociepłowni komunalnej, Ciepłownictwo, Ogrzewnictwo, Wentylacja.

[50] J. Skorek, W. Kostowski, Model pracy zasobnika ciepła zintegrowanego z małym układem skojarzonym, Prace Naukowe Politechniki Warszawskiej. Konferencje 3 (22) (2002) 1085–1092.

[51] W. KOSTOWSKI, J. KALINA, J. SKOREK, Zwiększenie efektywności energetycznej i ekonomicznej skojarzonego wytwarzania ciepła i energii elektrycznej przez zastosowanie zasobnika ciepła, Ciepłownictwo, Ogrzewnictwo, Wentylacja 36 (5) (2005) 8–14.

[52] J. SKOREK, W. KOSTOWSKI, Zasobniki ciepła w układach kogeneracyjnych—aspekty techniczne i ekonomiczne.

[53] S. Mańkowski, Projektowanie instalacji ciepłej wody użytkowej, Arkady, 1981.

[54] M. Dzierzgowski, Wymiana ciepła oraz dobór elementów układu płaskich kolektorów słonecznych z zasobnikiem ciepła, Ph.D. thesis, Politechnika Warszawska (1985).

[55] D. Mangold, Seasonal storage – a german success story, Sun & Wind Energy 1 (2007) 48–58.

[56] H.-F. Zhang, X.-S. Ge, H. Ye, Modeling of a space heating and cooling system with seasonal energy storage, Energy 32 (1) (2007) 51–58.

[57] H.-J. Diersch, D. Bauer, W. Heidemann, W. Rühaak, P. Schätzl, Finite element modeling of borehole heat exchanger systems: Part 1. fundamentals, Computers & Geosciences 37 (8) (2011) 1122–1135.

[58] H.-J. Diersch, D. Bauer, W. Heidemann, W. Rühaak, P. Schätzl, Finite element modeling of borehole heat exchanger systems: Part 2. numerical simulation, Computers & Geosciences 37 (8) (2011) 1136–1147.

[59] H. Paksoy, O. Andersson, S. Abaci, H. Evliya, B. Turgut, Heating and cooling of a hospital using solar energy coupled with seasonal thermal energy storage in an aquifer, Renewable Energy 19 (1) (2000) 117–122.

[60] J. Kim, Y. Lee, W. S. Yoon, J. S. Jeon, M.-H. Koo, Y. Keehm, Numerical modeling of aquifer thermal energy storage system, Energy 35 (12) (2010) 4955–4965.

[61] R. Cuypers, N. Maraz, J. Eversdijk, C. Finck, E. Henquet, H. Oversloot, H. v. Spijker, A. de Geus, Development of a seasonal thermochemical storage system, Energy Procedia 30 (2012) 207–214.

[62] H. Kerskes, B. Mette, F. Bertsch, S. Asenbeck, H. Drück, Chemical energy storage using reversible solid/gas-reactions (CWS)–results of the research project, Energy Procedia 30 (2012) 294–304.

[63] B. Mette, H. Kerskes, H. Drück, Concepts of long-term thermochemical energy storage for solar thermal applications–selected examples, Energy Procedia 30 (2012) 321–330.

[64] B. Michel, N. Mazet, S. Mauran, D. Stitou, J. Xu, Thermochemical process for seasonal storage of solar energy: Characterization and modeling of a high density reactive bed, Energy.

[65] J. Fan, S. Furbo, E. Andersen, Z. Chen, B. Perers, M. Dannemand, Thermal behavior of a heat exchanger module for seasonal heat storage, Energy Procedia 30 (2012) 244–254.

[66] T.-M. Tveit, T. Savola, A. Gebremedhin, C.-J. Fogelholm, Multi-period minlp model for optimising operation and structural changes to CHP plants in district heating networks with long-term thermal storage, Energy Conversion and Management 50 (3) (2009) 639–647.

[67] J. Milewski, M. Wołowicz, W. Bujalski, Seasonal thermal energy storage—a size selection, Applied Mechanics and Materials 467 (2014) 270...276.

[68] Hyprotech Corporation, HYSYS.Plant Steady State Modelling (1998).